



Cite this: *Catal. Sci. Technol.*, 2023, 13, 958

Received 2nd December 2022,  
Accepted 24th January 2023

DOI: 10.1039/d2cy02065c

rsc.li/catalysis

Commercially available iron salts  $\text{FeX}_2$  are remarkably active catalysts for pyrrolidine formation from organic azides *via* direct C–H bond amination. With  $\text{FeI}_2$ , amination is fast and selective, (<30 min for 80% yield at 2 mol% loading), TONs up to 370 are reached with just 0.1 mol% catalyst, different functional groups are tolerated, and a variety of C–H bonds were activated.

Since its discovery by Betley in 2013, intramolecular C–H amination using organic azides has become an attractive method for the synthesis of N-heterocycles.<sup>1</sup> This method allows the key step of the C–N bond formation to be highly atom economical, contrary to classical methods such as cross-coupling reactions, reductive elimination, and substitution reactions.<sup>2–6</sup> Following this pioneering work several other transition metal catalysts have been developed in the recent past for the intramolecular C–H amination with organic azides, including systems based on iron,<sup>1,7–16</sup> cobalt,<sup>17–21</sup> nickel,<sup>22,23</sup> ruthenium<sup>24,25</sup> and palladium.<sup>26,27</sup>

Iron-based catalysts are particularly active, and are of course also the most attractive due to the high abundance, low toxicity and low costs of the metal.<sup>28</sup> Although they require  $\text{Boc}_2\text{O}$  as additive to suppress product inhibition (Fig. 1).<sup>7</sup> While synthetically convenient, this addition significantly decreases the sustainability and atom-economy. Recently, we demonstrated that a mesoionic carbene ligand suppresses this product inhibition, providing a process that eliminates the necessity for product protection and that runs highly robustly with 7600 turnover numbers (TONs).<sup>14</sup> Despite these improvements, broad usability has been limited, in parts, by the multistep synthesis required to access the catalysts precursor.

The synthetic issue has been partially addressed with the development of  $\text{Fe}(\text{HMDS})_2$  as catalyst,<sup>8</sup> which is synthesized

in just one step from commercial sources (Fig. 1). We became particularly intrigued by blank measurements using commercially available  $\text{FeCl}_2$ , which revealed a mediocre 9% yield of pyrrolidine at 1 mol% loading.<sup>14</sup> Even though this yield is far from synthetically useful, it revealed catalytic activity that, in fact, is similar to that of Betley's pioneering Fe dipyrrin complex (Fig. 1; 9 vs. 5.7 TON). Based on these observations, we here report on  $\text{FeX}_2$  salts as convenient, commercially available, and air-stable catalyst precursors for the intramolecular C–H bond amination. We have benchmarked these salts in the preparation of different pyrrolidines, revealing high yields from organic azides

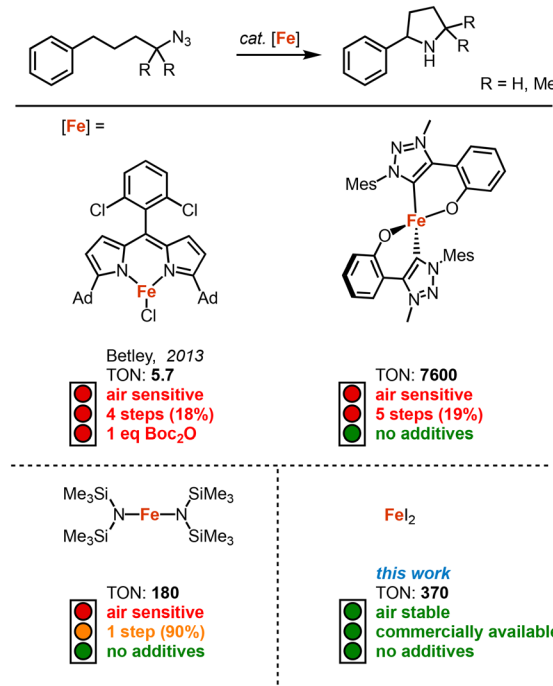


**Fig. 1** Selected examples of previously reported iron-based catalysts for the catalytic intramolecular C–H amination. The number of steps for the synthesis of the catalyst is represented with its total yield.

Department of Chemistry, Biochemistry and Pharmaceutical Sciences, University of Bern, Freiestrasse 3, CH-3012 Bern, Switzerland. E-mail: martin.albrecht@unibe.ch

† Electronic supplementary information (ESI) available. CCDC 2208587. For ESI and crystallographic data in CIF or other electronic format see DOI: <https://doi.org/10.1039/d2cy02065c>



without the need for any additives. This method therefore provides a remarkably sustainable and facile C–N bond formation protocol.

Our previous results showed that the model reaction of (4-azido-4-methylpentyl)benzene (**1a**) with 1 mol%  $\text{FeCl}_2$  resulted in a 9% yield of pyrrolidine **1b** after 6 h at 120 °C (Table 1, entry 1).<sup>14</sup> To optimize this process, the catalysis was run with an increased  $\text{FeCl}_2$  loading (10 mol%), which improved the yield of the amine product to 49% (entry 2). Moreover, significant amounts of the imine side product **1c** were formed (21%), which was characterized by a distinct multiplet in the  $^1\text{H}$  NMR spectrum at 7.75 ppm for the aryl proton in *para*-position. Also, trace amounts of enamine **1d** were observed, characterized by the allylic signal at 5.19 ppm. The overall yield for C–H bond activation is therefore around 70%. Notably, the tetrahydrate version of  $\text{FeCl}_2$ , gave a much lower 8% yield, suggesting that  $\text{H}_2\text{O}$  is detrimental to catalytic activity (entry 3). Based on the significant catalytic activity of  $\text{FeCl}_2$  at 10 mol% loading, a variety of iron salts were screened as catalyst precursors under these conditions.  $\text{FeBr}_2$  showed activity and selectivity similar to  $\text{FeCl}_2$  (entry 4). Interestingly, when exposing the reaction mixture to air with addition of pentane, colorless crystals suitable for X-ray analysis were obtained. The crystals were composed of the protonated amine **1b** with a bromide counterion, **1b**. $\text{HBr}$  (Fig. 2). We hypothesize that  $\text{HBr}$  is formed upon exposing the reactive iron catalyst to air, and subsequently trapped by the pyrrolidine **1b**. Using  $\text{FeI}_2$  instead of  $\text{FeCl}_2$  increased the yield of the amine substantially to 74% and lowered the amounts of imine and enamine by-products (Table 1, entry 5). In contrast, the iron salts  $\text{Fe(OAc)}_2$ ,  $\text{Fe(OTf)}_2$ ,  $\text{Fe(BF}_4\text{)}_2\cdot 6\text{H}_2\text{O}$  and  $\text{FeSO}_4\cdot 7\text{H}_2\text{O}$  did not show any detectable activity in C–H amination catalysis (entries 6–9).

Further catalytic optimization entailed the variation of the solvent (Table S1†), and, in particular, the  $\text{FeI}_2$  loading between 0.1 and 50 mol%. These experiments revealed a remarkable trend, as increasing the catalyst loading decreased the product yield (Table 2). Using 30–50 mol% of

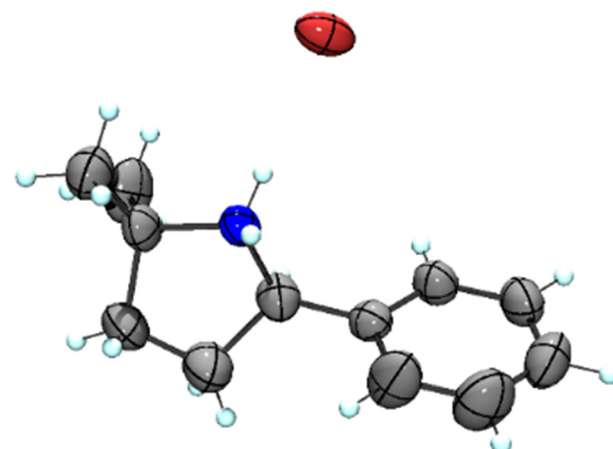


Fig. 2 Molecular structure from X-ray diffraction analysis of protonated amine **1b**. $\text{HBr}$  (50% probability ellipsoids).

catalyst resulted in full substrate conversion but only (sub) stoichiometric amounts of product (Table 2, entries 1–3). Upon lowering the catalyst loading to the 2–20 mol% range, full conversion is maintained, paired with a gradual increase in product yield from 52% to 83% as catalyst loading is lowered (entries 4–7). We attribute this unusual correlation of catalyst loading and product yield to the binding of either the azide substrate or, more likely, the product to the paramagnetic iron species. Such binding idles this fraction for  $^1\text{H}$  NMR integration and has also been observed with  $\text{Fe}(\text{HMDS})_2$ .<sup>8</sup> This model rationalizes the higher yields of cyclic amine observed at lower catalyst loadings. Further lowering of the catalyst loading to 0.5 and 0.1 mol% did not result in full conversion anymore and gave yields of 70% and 27%, respectively (entries 8–9). Extending the reaction time to 24 h with 0.1 mol%  $\text{FeI}_2$  increased the yield to 37%, yet a further increase of reaction time to 7 days did not improve the yield any further (entry 10). The maximum turnover number therefore is 370 under these conditions.

Table 1 Use of different commercially available iron salts for the intramolecular C–H amination<sup>a</sup>

Entry	Catalyst	Mol%		Yield <sup>b</sup> (%)			Total
				<b>1b</b>	<b>1c</b>	<b>1d</b>	
1 (ref. 14)	$\text{FeCl}_2$	1	<b>1a</b>	9	<2	n.d.	9
2	$\text{FeCl}_2$	10		49	21	<2	70
3	$\text{FeCl}_2\cdot 4\text{H}_2\text{O}$	10		8	<2	<2	8
4	$\text{FeBr}_2$	10		48	17	<2	65
5	$\text{FeI}_2$	10		74	6	<2	80
6	$\text{Fe(OAc)}_2$	10		n.d.	n.d.	n.d.	0
7	$\text{Fe(OTf)}_2$	10		n.d.	n.d.	n.d.	0
8	$\text{Fe(BF}_4\text{)}_2\cdot 6\text{H}_2\text{O}$	10		n.d.	n.d.	n.d.	0
9	$\text{FeSO}_4\cdot 7\text{H}_2\text{O}$	10		n.d.	n.d.	n.d.	0

<sup>a</sup> Catalysis was performed on a 0.25 mmol scale in J Young NMR tubes; see ESI† for exact experimental details. <sup>b</sup> Yields and conversions were determined by  $^1\text{H}$  NMR spectroscopy using 1,3,5-trimethoxybenzene as internal standard.



**Table 2** Effect of different loadings of  $\text{FeI}_2$  on the catalytic intramolecular C–H amination

Entry <sup>a</sup>	$\text{FeI}_2$ (mol%)	<b>1b</b>	
		Yield <b>1b</b> (%)	Conversion <sup>b</sup> (%)
1	50	8	98
2	40	18	98
3	30	33	98
4	20	52	98
5	10	74	98
6	5	81	96
7	2	83	97
8	0.5	70	86
9	0.1	27	29
10 <sup>c</sup>	0.1	37	49

<sup>a</sup> Catalysis was performed on a 0.25 mmol scale in J Young NMR tubes; see ESI† for exact experimental details. <sup>b</sup> Yields and conversions were determined by  $^1\text{H}$  NMR spectroscopy using 1,3,5-trimethoxybenzene as internal standard. <sup>c</sup> Reaction time was increased to 24 h.

To get more insight into the catalytic activity of  $\text{FeI}_2$  at low catalyst loading, the reaction was followed by  $^1\text{H}$  NMR spectroscopy. After heating at 120 °C for 5 min using 5 mol%  $\text{FeI}_2$ , the yield was 26%, corresponding to an initial turnover frequency (TOF) of at least 60  $\text{h}^{-1}$  (Fig. S2†). In comparison, the highest TOF observed for this transformation is 150  $\text{h}^{-1}$  using 1 mol% of a mesoionic carbene iron complex.<sup>14</sup> The catalytic rate then gradually slows down as expected for a first order reaction. Mechanistically,  $\text{FeI}_2$  may operate similar to other iron catalysts *via* imidyl/nitrene formation and subsequent hydrogen atom abstraction and sequential or concerted C–N bond formation.<sup>8,20–22</sup> In agreement with the involvement of an open-shell species, conversion was completely stalled when TEMPO was added to a catalytic run at early reaction stages (14% conversion). Though other scenarios like coordination by TEMPO or iron oxidation obviously may also cause this effect.

To benchmark  $\text{FeI}_2$  as a C–H amination catalyst against known iron catalysts, a set of standard organic azide substrates with diverse substitution patterns were evaluated (Fig. 3). Primary azides are not suitable substrates as azide **2a** did not form any detectable pyrrolidine and instead, a mixture of unidentified products was obtained. Primary azides are known to be challenging substrates, as the protons in the  $\alpha$ -position can undergo a hydrogen atom abstraction (HAA) upon formation of the nitrene.<sup>29</sup> This limitation has been observed with some, but not all,<sup>1,7,9–11,16</sup> previously developed Fe catalysts.<sup>14,22</sup>

In contrast,  $\text{FeI}_2$  catalyzes the C–H amination with a variety of tertiary azides. Substituting the *para*-position of the model substrate by a Me, OMe, Br or a thiophene group resulted in a 70–81% yield of the cyclic amine (**3b**–**6b**) after 30 min. The activity is similar to **1b** and suggests only a minor influence of aromatic substituents on the amination reactivity. Activation

of a primary rather than secondary benzylic C–H bond as in substrate **7a** did not lead to any detectable amount of the corresponding indolidine. Instead, mainly starting material was observed, with small unidentified impurities, even after prolonged reaction times (6 h). This reactivity contrasts with the high conversion of this substrate with iron catalysts that contain chelating ligands.<sup>1,7,8,14</sup> Expanding the alkyl chain by one methylene group (substrate **8a**) selectively affords the pyrrolidine **8b** (37% after 6 h), while no signals were detected for a piperidine homologue that would result from benzylic C–H bond activation. This result indicates that the reaction is kinetically controlled to give the 5-membered heterocycle, rather than producing the less ring-strained 6-membered piperidine from activation of the weaker benzylic C–H bond.<sup>30</sup> This selectivity is identical to that of other homogeneous iron catalysts containing robustly bound ligands,<sup>8,14</sup> yet distinct from other catalytic systems that tend to afford mixtures of both heterocycles.<sup>31</sup> Intrigued by the ability of  $\text{FeI}_2$  as a precatalyst for the activation of the strong aliphatic C–H bond in **8a**, other aliphatic substrates were evaluated. The tertiary aliphatic C–H bond in **9a** is poorly aminated, producing the aliphatic pyrrolidine **9b** only in trace amounts even after longer reaction times. Secondary and primary aliphatic C–H bonds are unreactive and **10a** and **11a** did not lead to any

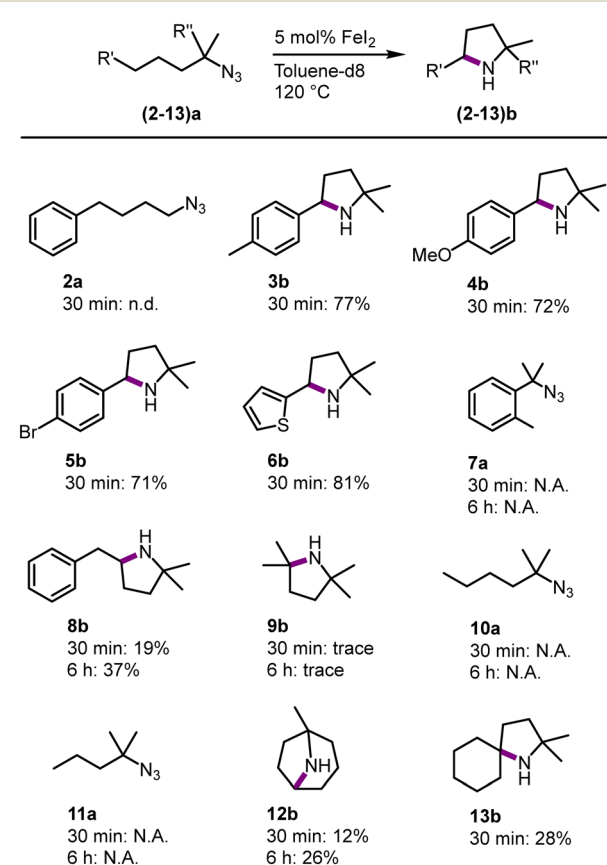


**Fig. 3** Substrate scope of the intramolecular C–H amination using 5 mol% of  $\text{FeI}_2$  in toluene-d<sub>8</sub> at 120 °C, spectroscopic yields determined by  $^1\text{H}$  NMR spectroscopy using 1,3,5-trimethoxybenzene as internal standard.



cyclized product. Remarkably, tertiary and even secondary aliphatic C–H bonds are activated when using substrates **12a** and **13a**, respectively. While these C–H bond strengths are comparable to those in **9a** and **10a**, respectively, the amine product is sterically more protected. This distinct reactivity pattern may point to product inhibition, which is expected to be more relevant with less sterically shielded amines and with catalysts containing small and kinetically labile ligands. Indeed, the introduction of bidentate mesoionic carbene ligands at the iron center efficiently suppresses such inhibition.<sup>14</sup> Mimicking this effect by adding exogeneous ligands such as pyridine, bipyridine, or  $\text{PPh}_3$  did not improve conversion, or even suppressed activity completely (bi- or terpyridine; Table S2†). Overall,  $\text{FeI}_2$  has considerable limitations as a catalyst for the amination of unshielded aliphatic C–H bonds, though it offers an attractive alternative to sophisticated iron complexes for the amination of benzylic C–H bonds as well aliphatic C–H bonds that are producing sterically rather shielded amine products. It may therefore become a viable methodology for the construction of the pyrrolidine motif in agrochemical and pharmaceutical products with this motif.<sup>32–36</sup>

In conclusion, a convenient and sustainable method is described for the synthesis of pyrrolidines from organic azides through direct C–H amination using  $\text{FeI}_2$  as a cheap, commercially available, and air-stable catalyst. Low catalyst loadings accomplish the synthesis of these N-heterocycles in high yields with low reaction times. Some functional groups are tolerated by this catalyst, and activation of benzylic C–H bonds is considerably more efficient than activation of stronger aliphatic C–H bonds. The latter requires sterically congested pyrrolidine products to be formed in order to limit product inhibition. The convenience of an air-stable and commercial catalyst is attractive for implementing C–H amination as a method for pyrrolidine synthesis both for organic synthesis and industrial applications.

## Author contributions

W. S. and L. H. performed the work and analysed the data. W. S. and M. A. conceived the project and wrote the manuscript. M. A. supervised the project.

## Conflicts of interest

There are no conflicts to declare.

## Acknowledgements

We thank the Xray crystal structure determination service unit of the Department of Chemistry, Biochemistry and Pharmaceutical Sciences of the University of Bern for crystallographic analyses. Generous financial support from SNSF (20020\_182633) and ERC (CoG 615653) as well as an International Mobility Grant of the French Ministry of Higher Education (to L. H.) are acknowledged.

## Notes and references

- 1 E. T. Hennessy and T. A. Betley, *Science*, 2013, **340**, 591–595.
- 2 J. Bariwal and E. Van Der Eycken, *Chem. Soc. Rev.*, 2013, **42**, 9283–9303.
- 3 N. R. Candeias, L. C. Branco, P. M. P. Gois, C. A. M. Afonso and A. F. Trindade, *Chem. Rev.*, 2009, **109**, 2703–2802.
- 4 A. Deiters and S. F. Martin, *Chem. Rev.*, 2004, **104**, 2199–2238.
- 5 S. H. Cho, J. Y. Kim, J. Kwak and S. Chang, *Chem. Soc. Rev.*, 2011, **40**, 5068–5083.
- 6 P. V. Kattamuri, J. Yin, S. Siriwongsup, D. H. Kwon, D. H. Ess, Q. Li, G. Li, M. Yousufuddin, P. F. Richardson, S. C. Sutton and L. Kürti, *J. Am. Chem. Soc.*, 2017, **139**, 11184–11196.
- 7 B. Bagh, D. L. J. Broere, V. Sinha, P. F. Kuijpers, N. P. Van Leest, B. De Bruin, S. Demeshko, M. A. Siegler and J. I. Van Der Vlugt, *J. Am. Chem. Soc.*, 2017, **139**, 5117–5124.
- 8 W. Stroek and M. Albrecht, *Chem. Sci.*, 2023, DOI: [10.1039/d2sc04170g](https://doi.org/10.1039/d2sc04170g).
- 9 K. P. Shing, Y. Liu, B. Cao, X. Y. Chang, T. You and C. M. Che, *Angew. Chem., Int. Ed.*, 2018, **57**, 11947–11951.
- 10 Y. D. Du, Z. J. Xu, C. Y. Zhou and C. M. Che, *Org. Lett.*, 2019, **21**, 895–899.
- 11 Y. D. Du, C. Y. Zhou, W. P. To, H. X. Wang and C. M. Che, *Chem. Sci.*, 2020, **11**, 4680–4686.
- 12 S. Liang, X. Zhao, T. Yang and W. Yu, *Org. Lett.*, 2020, **22**, 1961–1965.
- 13 T. You, S. H. Zeng, J. Fan, L. Wu, F. Kang, Y. Liu and C. M. Che, *Chem. Commun.*, 2021, **57**, 10711–10714.
- 14 W. Stroek, M. Keilwerth, D. M. Pividori, K. Meyer and M. Albrecht, *J. Am. Chem. Soc.*, 2021, **143**, 20157–20165.
- 15 N. C. Thacker, Z. Lin, T. Zhang, J. C. Gilhula, C. W. Abney and W. Lin, *J. Am. Chem. Soc.*, 2016, **138**, 3501–3509.
- 16 D. A. Iovan, M. J. T. Wilding, Y. Baek, E. T. Hennessy and T. A. Betley, *Angew. Chem., Int. Ed.*, 2017, **56**, 15599–15602.
- 17 P. F. Kuijpers, M. J. Tiekkink, W. B. Breukelaar, D. L. J. Broere, N. P. van Leest, J. I. van der Vlugt, J. N. H. Reek and B. de Bruin, *Chem. – Eur. J.*, 2017, **23**, 7945–7952.
- 18 M. Goswami, P. Geuijen, J. N. H. Reek and B. de Bruin, *Eur. J. Inorg. Chem.*, 2018, 617–626.
- 19 Y. Baek, E. T. Hennessy and T. A. Betley, *J. Am. Chem. Soc.*, 2019, **141**, 16944–16953.
- 20 Y. Baek and T. A. Betley, *J. Am. Chem. Soc.*, 2019, **141**, 7797–7806.
- 21 Y. Baek, A. Das, S. L. Zheng, J. H. Reibenspies, D. C. Powers and T. A. Betley, *J. Am. Chem. Soc.*, 2020, **142**, 11232–11243.
- 22 Y. Dong, R. M. Clarke, G. J. Porter and T. A. Betley, *J. Am. Chem. Soc.*, 2020, **142**, 10996–11005.
- 23 Y. Dong, C. J. Lund, G. J. Porter, R. M. Clarke, S. L. Zheng, T. R. Cundari and T. A. Betley, *J. Am. Chem. Soc.*, 2021, **143**, 817–829.
- 24 J. Qin, Z. Zhou, T. Cui, M. Hemming and E. Meggers, *Chem. Sci.*, 2019, **10**, 3202–3207.
- 25 Z. Zhou, S. Chen, J. Qin, X. Nie, X. Zheng, K. Harms, R. Riedel, K. N. Houk and E. Meggers, *Angew. Chem., Int. Ed.*, 2019, **58**, 1088–1093.



26 D. L. J. Broere, B. De Bruin, J. N. H. Reek, M. Lutz, S. Dechert and J. I. Van Der Vlugt, *J. Am. Chem. Soc.*, 2014, **136**, 11574–11577.

27 D. L. J. Broere, N. P. Van Leest, B. De Bruin, M. A. Siegler and J. I. Van Der Vlugt, *Inorg. Chem.*, 2016, **55**, 8603–8611.

28 T. Keijer, V. Bakker and J. C. Slootweg, *Nat. Chem.*, 2019, **11**, 190–195.

29 Y. Dong, J. T. Lukens, R. M. Clarke, S. L. Zheng, K. M. Lancaster and T. A. Betley, *Chem. Sci.*, 2020, **11**, 1260–1268.

30 Y.-R. Luo, *Comprehensive Handbook of Chemical Bond Energies*, CRC Press, Taylor & Francis Group, Boca Raton, 2007.

31 A. E. Bosnidou and K. Muñiz, *Angew. Chem., Int. Ed.*, 2019, **58**, 7485–7489.

32 D. O'Hagan, *Nat. Prod. Rep.*, 2000, **17**, 435–446.

33 A. R. Pinder, *Nat. Prod. Rep.*, 1984, **4**, 225–230.

34 R. Hili and A. K. Yudin, *Nat. Chem. Biol.*, 2006, **2**, 284–287.

35 E. Vitaku, D. T. Smith and J. T. Njardarson, *J. Med. Chem.*, 2014, **57**, 10257–10274.

36 R. D. Taylor, M. MacCoss and A. D. G. Lawson, *J. Med. Chem.*, 2014, **57**, 5845–5859.